Preprints of the 19th World Congress
The International Federation of Automatic Control
Cape Town, South Africa. August 24-29, 2014

Robust Trajectory Tracking for Underactuated VTOL Aerial Vehicles: Extended for Adaptive Disturbance Compensation ⋆

Paolo Castaldi * Nicola Mimmo * Roberto Naldi * Lorenzo Marconi *

* *Department of Electrical, Electronic and Information Engineering, University of Bologna, Bologna, 40133, Italy,*
{`paolo.castaldi, nicola.mimmo2, roberto.naldi, lorenzo.marconi` } `@unibo.it`.

Abstract: This work proposes a feedback control strategy to let the dynamics of an under-actuated Vertical Take-Off and Landing (VTOL) aerial vehicle to track a desired trajectory thanks to an adaptive robust compensation of the aerodynamic disturbances. The novelty of the proposed approach consists in employing an aerodynamic disturbance observer derived using the NonLinear Geometric Approach and Radial Basis Functions (RBF). The obtained estimation is directly employed by a nonlinear robust feedback law which relies on a cascade control paradigm in which the attitude dynamics and the position dynamics of the vehicle play the role of the inner and of the outer loop, respectively. The robustness of the proposed approach is also demonstrated by means of simulation results in which the aerodynamic model of a multi-propeller aircraft is considered.

Keywords: Adaptive Flight Control; Geometric Approach; Radial Basis Function; Disturbance Estimation; Quad-rotor.

1. INTRODUCTION

Due to their agility and high level of maneuverability, miniature Vertical Take-Off and Landing (VTOL) aerial vehicles are currently employed successfully in a large number of applications ranging from surveillance, data harvesting, search and rescue operations Feron and Johnson [2008] or even to perform advanced robotic tasks Marconi and Naldi [2012]. To exploit the potential of such a kind of machines, an important role is played by the design of the control law.

Several contributions and seminal papers document different approaches to the control design for such a class of under-actuated systems Hauser et al. [1992], Martin et al. [1996]. More recently, different nonlinear control techniques have been employed to improve the stability properties of the vehicle. In Hua et al. [2009], Lyapunov based techniques are shown to obtain almost-global stability of the system dynamics and robustness to aerodynamic drag disturbances. Adaptive control algorithms and output feedback approaches have been considered for instance in Abdessameud and Tayebi [2010] and Marconi et al. [2013]. Backstepping control design has been proposed in Frazzoli et al. [2000] in order to perform aggressive maneuvers, while globally stabilizing control laws, based on hybrid systems techniques, have appeared in Casau et al. [2013] and Naldi et al. [2013]. Finally, a survey describing feedback control design for under-actuated VTOL systems has appeared in Hua et al. [2013].

One of the most successful VTOL configuration is given by the quad-rotor aerial vehicle Mahony et al. [2012]. Generally speaking the quad-rotor model is composed of:

- the rigid body equations (linear and angular accelerations);
- the description of external forces (gravity, propeller forces, body aerodynamic effects) and momentum (propeller RPM variation, propeller and body aerodynamic damping effects, gyroscopic effects).

While the rigid body model as well as the gravity contribution are described by a well known set of equations, the external aerodynamic forces and momentum can be only approximated. Accordingly, this paper proposes an adaptive control law composed of two different parts. The former consists of a robust stabilizing controller that is designed by taking advantage of the knowledge of the reliable part of the quad–rotor model (rigid body and gravity). The latter is given by an adaptive estimation law, designed using Radial Basis Functions Neural Network (RBF NN), that allows to compensate for model uncertainties and generic time varying external disturbances. As a result, the performances of the closed-loop system are improved with respect to other existing approaches in which only constant

⋆ This research has been framed within the collaborative project SHERPA (ICT 600958) supported by the European Community under the 7th Framework Programme. Corresponding author: Roberto Naldi, `roberto.naldi@unibo.it`.

disturbances are considered (see Cabecinhas et al. [2014] among others).

The adaptive estimation is based on the NonLinear Geometric Approach and the Radial Basis Function. In recent years the Non-Linear Geometric Approach (NLGA) De Persis and Isidori [2001] has been efficiently used to isolate faults and external disturbances Baldi et al. [2011, 2013b], Castaldi et al. [2010]. In particular, in this paper the NLGA has been exploited to to single out three new scalar sub–systems at the basis of the estimation filter design. In particular, the NLGA allows the computation of a coordinate change in the state and output spaces leading to new subsystems affected, in turn, only by one of the three external force components, as described in Section 4. Hence, independent estimation filters can be designed and, in particular, due to disturbance components generic time behavior, this paper exploits also the application of Radial Basis Function (RBF), very useful to estimate generic time signals.

The paper is organised as follows. Section 2 describes the dynamic model exploited during both the controller and the estimators design phases. Section 3 shows the controller design process, how the estimation is exploited into the control law and the overall closed-loop system stability. Section 4 highlights the procedures and the results obtained in terms of adaptive filters for disturbance estimation. The performance of the estimation scheme and of the overall controller are shown in the figures of Section 5. Finally, Section 6 contains the conclusion.

1.1 Notation

Throughout this paper, $\mathcal{F}_i$ and $\mathcal{F}_b$ denote, respectively, an inertial reference frame and a reference frame attached to the center of gravity of the vehicle. With $I_n \in \mathbb{R}^{n\times n}$ we denote the n-dimensional identity matrix. With e_1, e_2 and e_3 we denote the unit vectors $e_1 := [1, 0, 0]^T$, $e_2 := [0, 1, 0]^T$ and $e_3 := [0, 0, 1]^T$. For any $x \in \mathbb{R}^3$, we let

$$S(x) := \begin{bmatrix} 0 & -x_3 & x_2 \\ x_3 & 0 & -x_1 \\ -x_2 & x_1 & 0 \end{bmatrix}$$

be a skew-symmetric matrix and we denote with $^\wedge$ the inverse operator such that $S(x)^\wedge = x$. Given a rotation matrix $R \in SO(3)$, $\Theta(R) := \frac{1}{2}\text{trace}(I_3 - R)$. With S_n we denote the n-dimensional unit sphere defined as $S_n := \{x \in \mathbb{R}^{n+1} : \|x\| = 1\}$. A unit quaternion $q \in S_3$ is defined as a pair $q = [\eta, \epsilon^T]^T$ in which $\eta \in \mathbb{R}$ and $\epsilon \in \mathbb{R}^3$ are denoted respectively as the scalar and vector part. Given unit quaternions $q_1 = [\eta_1, \epsilon_1^T]^T$ and $q_2 = [\eta_2, \epsilon_2^T]^T$, the standard quaternion product is defined as

$$q_1 \otimes q_2 = \begin{bmatrix} \eta_1 & -\epsilon_1^T \\ \epsilon_1 & \eta_1 I_3 + S(\epsilon_1) \end{bmatrix} \begin{bmatrix} \eta_2 \\ \epsilon_2 \end{bmatrix} .$$

With $\mathbf{1} = [1, 0, 0, 0]^T \in S_3$ we denote the identity quaternion element and, for a quaternion $q = [\eta, \epsilon^T]^T \in S_3$, with $q^{-1} = [\eta, -\epsilon^T]^T$ the inverse, so that $q \otimes q^{-1} = q^{-1} \otimes q = \mathbf{1}$.

We refer to a *saturation function* as a mapping $\sigma : \mathbb{R}^n \to \mathbb{R}^n$ such that, for $n = 1$,

(1) $|\sigma'(s)| := |d\sigma(s)/ds| \leq 2$ for all s,
(2) $s\sigma(s) > 0$ for all $s \neq 0$, $\sigma(0) = 0$,
(3) $\sigma(s) = \text{sgn}(s)$ for $|s| \geq 1$,
(4) $|s| < |\sigma(s)| < 1$ for $|s| < 1$.

For $n > 1$, the properties listed above are intended to hold componentwise.

2. DYNAMIC MODEL

The dynamics of a large class of miniature Vertical Take-Off and Landing (VTOL) aerial vehicles, including helicopters, ducted-fan and multi-propeller configurations, can be described by considering the so called *vectored-thrust* (see among others Hua et al. [2013], Abdessameud and Tayebi [2010]) dynamic model:

$$\begin{aligned} M\ddot{p} &= -u_f Re_3 + Mge_3 + d_f \\ \dot{R} &= RS(w) \\ J\dot{w} &= S(Jw)w + u_\tau \end{aligned} \tag{1}$$

in which $p = [x, y, z]^T \in \mathbb{R}^3$ denotes the position of the center of gravity of the system expressed in the inertial reference frame $\mathcal{F}_i$, $w = [w_x, w_y, w_z]^T \in \mathbb{R}^3$ is the angular speed expressed in the body frame $\mathcal{F}_b$, $R \in SO(3)$ is the rotation matrix relating vectors in $\mathcal{F}_b$ to vectors in $\mathcal{F}_i$, $M \in \mathbb{R}_>$ and $J \in \mathbb{R}^{3\times3}$ (with the property that $J = J^T > 0$) are the mass and the inertia matrix of the system, $u_f \in \mathbb{R}_{\geq 0}$ denotes the control force generated by the aircraft own actuators (which, by construction, is directed along the body z axis) and $u_\tau \in \mathbb{R}^3$ is the control torque vector. The force vector $d_f \in \mathbb{R}^3$ models the presence of aerodynamic force disturbances: see Section 2.1 for a description.

Rotations can be parameterized by means of a unit quaternion $q \in S_3$ through the mapping $\mathcal{R} : S_3 \to SO(3)$ (known as Rodriguez formula Shuster [1993]) defined as

$$\mathcal{R}(q) = I + 2\eta S(\epsilon) + 2S(\epsilon)^2 .$$

By employing the quaternion parametrization, the dynamics equation (1) is rewritten as

$$\begin{aligned} M\ddot{p} &= -u_f \mathcal{R}(q)e_3 + Mge_3 + d_f \\ \dot{q} &= \frac{1}{2} q \otimes \begin{bmatrix} 0 \\ w \end{bmatrix} \\ J\dot{w} &= S(Jw)w + u_\tau . \end{aligned} \tag{2}$$

2.1 External Disturbances Modelisation

Based on several works available in literature (see also Mahony et al. [2012] and references therein) this paper implements, only for simulation purposes (the controller does not know the following model), the two main external forces effects: the actual propeller thrust and the body drag.

The body drag force vector can be easily modeled by:

$$F_{BD} = -\frac{1}{2}\rho S |V_a|^2 C_D \frac{V_a}{|V_a|}, \quad V_a = V_I - W \tag{3}$$

where the airspeed vector, V_a, is equal to the difference between the body inertial speed vector, V_I, and the wind speed vector, W. Hence, this force vector is employed to simulate both the effects of the translation in clean air and the drag due to the wind field during hovering fights.

The second main external force contribution is due to the difference between the nominal and actual propeller thrust. The simplified model for controller design assumes that thrust is proportional to the square of propeller angular rate without any influence from the flight conditions. This is clearly not true and the difference between the nominal and actual thrust can be described by the following equations:

$$\begin{aligned} F_{\Delta T} &= R' e_3 \Delta T \\ \Delta T &= T_{ideal} - T_{actual} \\ T_{ideal} &= \rho n^2 D^4 C_T(0) \\ T_{actual} &= \rho n^2 D^4 C_T(J) \\ J &= -\frac{w_a}{nD} \end{aligned} \tag{4}$$

where the advance ratio, J, is a function of the z-body airspeed, w_a, and of the propeller turn rate, n. The term C_T represent the thrust coefficient (available from wind tunnel test).

The terms F_{BD} and $F_{\Delta T}$ represent the two main contributions to d_f, *i.e.* $d_f = F_{BD} + F_{\Delta T} + ...$

3. CONTROL LAW

3.1 Control Goal

The goal of the control law to be designed is to track a given time reference position and orientation

$$p_R(t) \in \mathbb{R}^3, \quad R_R(t) \in SO(3) \tag{5}$$

assuming full knowledge of the state of the system. The desired references (5) must be chosen to satisfy the *functional controllability* constraints of the system by considering the special case in which the unknown exogenous disturbances d_f and d_τ are zero. More specifically, following Naldi et al. [2013], we define the *reference control force vector* v_R^c required to track the desired position trajectory as

$$v_R^c(\ddot{p}_R) := Mge_3 - M\ddot{p}_R\,, \tag{6}$$

and, accordingly, the reference attitude $R_R(t) \in SO(3)$ must then satisfy

$$R_R e_3 = \frac{v_R^c(\ddot{p}_R)}{\|v_R^c(\ddot{p}_R)\|}\,. \tag{7}$$

From a geometrical viewpoint, the above constraint requires the body z-axis of the vehicle to be aligned with the reference control force vector.

Note that solutions to (7) are nonunique. In fact the constraint is fixing only two of the three degrees of freedom characterizing the rotation matrix (see also Casau et al. [2013], Frazzoli et al. [2000]). Moreover, to compute a solution to (7), the reference control force vector should be such that

$$\|v_R^c(\ddot{p}_R(t))\| > v^L, \ \forall t \geq 0 \tag{8}$$

for some $v^L > 0$. The force and torque control inputs required to track asymptotically the desired position and orientation (in the absence of the exogenous disturbances d_f and d_τ) are then given by

$$u_{f_R} = \|v_R^c(\ddot{p}_R)\|, \ u_{\tau_R} = J\dot{w}_R - S(Jw_R)w_R, \tag{9}$$

where $w_R := R_R^T \dot{R}_R{}^\wedge$ is the reference angular velocity. Finally, $p_R(t)$ and $R_R(t)$ are required to be sufficiently smooth functions of time satisfying appropriate bounds on high order derivatives.

3.2 Position Control Law

Let us consider the position dynamics in (1). By considering the following error coordinates

$$\bar{p} := p - p_R, \qquad \dot{\bar{p}} := \dot{p} - \dot{p}_R,$$

the position error dynamics can be written as

$$M\ddot{\bar{p}} = -u_f R e_3 + Mge_3 - M\ddot{p}_R + d_f\,. \tag{10}$$

To stabilize the origin of (10), we define the *control force vector* as

$$v^c(\bar{p}, \dot{\bar{p}}, \ddot{p}_R, \hat{d}_f) := v_R^c(\ddot{p}_R) + \kappa(\bar{p}, \dot{\bar{p}}) + \hat{d}_f\,, \tag{11}$$

with $\kappa(\bar{p}, \dot{\bar{p}})$ a static state feedback law such that $\kappa(0,0) = 0$ and where $\hat{d}_f$ is the available estimation for the exogenous disturbance d_f. From (11) it is possible to compute the control orientation $R_c := R_R R_c'(\bar{p}, \dot{\bar{p}}, \hat{d}_f)$, with $R_c'(\bar{p}, \dot{\bar{p}}, \hat{d}_f) \in SO(3)$ such that

$$R_c'(0,0,0) = I_3, \quad R_c'(\bar{p}, \dot{\bar{p}}, \hat{d}_f)e_3 = R_R^T \frac{v^c(\bar{p}, \dot{\bar{p}}, \ddot{p}_R, \hat{d}_f)}{\|v^c(\bar{p}, \dot{\bar{p}}, \ddot{p}_R, \hat{d}_f)\|}\,. \tag{12}$$

Moreover, it is also possible to define the control angular speed as $w_c := R_c^T \dot{R}_c{}^\wedge$. Note that, when $\bar{p} = \dot{\bar{p}} = \hat{d}_f = 0$ the control orientation R_c coincides with the reference attitude R_R. To avoid singularities in (12), a suitable design of the position control law $\kappa(\bar{p}, \dot{\bar{p}})$ and of the filter generating the estimated value of the exogenous disturbances $\hat{d}_f$ is required so as to guarantee that the magnitude of the force control vector (6) is non vanishing regardless the current position and velocity errors. In particular, let $\bar{v}_{fb}, \bar{v}_d \in \mathbb{R}_{>0}$ such that

$$\bar{v}_{fb} + \bar{v}_d < v^L. \tag{13}$$

As far as $\hat{d}_f$ is concerned, the following constraint is obtained by properly designing the filter (i.e. by introducing a saturation in the estimation value employed directly by the control law)

$$|\hat{d}_f|_\infty \leq \bar{v}_d\,. \tag{14}$$

As far as the position stabilizer $\kappa(\cdot)$ is concerned, drawing inspiration from [Isidori et al., 2003, Appendix C], we focus on the following nested saturation feedback law

$$\begin{aligned} &\zeta_1 := \bar{p}, \quad \zeta_2 := \dot{\bar{p}} + \lambda_1 \sigma\left(\frac{k_1}{\lambda_1}\zeta_1\right) \\ &\kappa(\bar{p}, \dot{\bar{p}}) \ := \lambda_2 \sigma\left(\frac{k_2}{\lambda_2}\zeta_2\right) \end{aligned} \tag{15}$$

in which λ_1, λ_2, k_1 and k_2 are chosen as

$$\lambda_i = \varepsilon^{(i-1)}\lambda_i^\star, \qquad k_i = \varepsilon\, k_i^\star, \qquad i = 1,2 \tag{16}$$

where $k_i^\star$, $\lambda_i^\star$ are positive constants fixed as (see also [Isidori et al., 2003, Appendix C])

$$\frac{\lambda_2^\star}{k_2^\star} < \frac{\lambda_1^\star}{4}, \quad 4k_1^\star\lambda_1^\star < \frac{\lambda_2^\star}{4}, \quad 6\frac{k_1^\star}{k_2^\star} < \frac{1}{24} \tag{17}$$

and ε is an arbitrary positive number. Note that, by the definition of saturation function, $\|\kappa(\cdot)\| \leq \sqrt{3}\,\lambda_2^\star\varepsilon$ hence - by considering (11), (13) and (14) - the constraint $\|v^c(\cdot)\| > 0$ holds true by choosing

$$\varepsilon \leq \bar{v}_{fb}/\sqrt{3}\lambda_2^\star \tag{18}$$

Finally, the control input u_f is fixed as

$$u_f = u_{f_c}(\bar{p}, \dot{\bar{p}}, \ddot{p}_R, \hat{d}_f) := \|v^c(\bar{p}, \dot{\bar{p}}, \ddot{p}_R, \hat{d}_f)\|\,. \tag{19}$$

3.3 Attitude Control Law

Let us denote with $q_R, q_c \in S_3$, where $\mathcal{R}(q_R) \equiv R_R$ and $\mathcal{R}(q_c) \equiv R_c$ for all $t \geq 0$, the *reference* and *control quaternion*, respectively. In particular q_R and q_c can be obtained by lifting trajectories in $SO(3)$ to trajectories in S_3 by employing the path-lifting mechanism proposed in Mayhew et al. [2012].

Let us define the following attitude error coordinates

$$\bar{q} = q_c^{-1} \otimes q, \; \hat{w} := w - \bar{w}_R \tag{20}$$

with $\bar{w}_R := \mathcal{R}(\bar{q})^T w_R$. The attitude error dynamics can be then written as

$$\begin{aligned} \dot{\bar{q}} &= \frac{1}{2}\bar{q} \otimes \begin{bmatrix} 0 \\ \hat{w} \end{bmatrix} + \Gamma_q(\bar{q}, y_\zeta) \\ J\dot{\hat{w}} &= \Sigma'(\hat{w}, \bar{w}_R)\hat{w} + S(J\bar{w}_R)\bar{w}_R + JS(\bar{w}_R - \bar{w}_c)\bar{w}_R + \\ &\quad + u_\tau - J\mathcal{R}(\bar{q})^T \dot{w}_R \,. \end{aligned} \tag{21}$$

in which

$$\Gamma_q(\bar{q}, y_\zeta) = -\frac{1}{2}\bar{q} \otimes \begin{bmatrix} 0 \\ \mathcal{R}(\bar{q})^T y_\zeta \end{bmatrix} \tag{22}$$

with $y_\zeta := w_c - w_R$ and where $\Sigma'(\hat{w}, \bar{w}_R)$ is a skew-symmetric matrix defined as $\Sigma'(\hat{w}, \bar{w}_R) := S(J\hat{w}) + S(J\bar{w}_R) - (S(\bar{w}_R)J + JS(\bar{w}_R))$.

For the above system, we consider the following attitude controller

$$u_\tau = u_{\tau_R} + u_\tau^{FB}(\bar{q}, \hat{w}) \tag{23}$$

where u_{τ_R} is defined in (9) and with

$$u_\tau^{FB}(\bar{q}, \hat{w}) = -K_P\bar{\epsilon} - K_P K_D \hat{w} \tag{24}$$

in which K_P, K_D are positive gains.

Note that the attitude subsystem (21) is affected by the closed-loop position error dynamics (10), through the input y_ζ, and by the exogenous disturbance d_τ.

3.4 Overall Closed-Loop System

By considering the overall position and attitude controllers (19) and (24), following the results given in ([Isidori et al., 2003, Proposition 5.7.1]) and (Naldi et al. [2013]), it is possible to prove the following result.

Proposition 1. Let us consider system (2) in which the control inputs u_f and u_τ are designed as in (19) and (24). For the position controller, let k_1, k_2, λ_1, λ_2 be chosen as (16)-(17), and let $\varepsilon > 0$ be such that (18) holds. Let $|d_\tau|_\infty < D_\tau$, $|d_f|_\infty < D_f$ and $\hat{d}_f$ such that (14) for some $D_f, D_\tau \in \mathbb{R}_{>0}$. Then, there exist $K_D^\star$, $K_P^\star$ such that for all $K_D < K_D^\star$, $K_P > K_P^\star$

$$\limsup_{t\to\infty} \|(p - p_R, \, q - q_R)\| \leq \gamma(d_f - \hat{d}_f)\,.$$

In the special case in which the estimate $\hat{d}_f$ converges to the disturbance d_f, the above proposition shows how the tracking of the desired references becomes asymptotic. This is clearly one important advantage achieved by estimating the value of d_f. On the other hand, when $\hat{d}_f \neq d_f$, if the restrictions on the exogenous inputs are satisfied, practical tracking is still achieved.

4. EXTERNAL DISTURBANCES ESTIMATION

This section recalls the design methodology and the implementation scheme of the NLGA RBF-NN based filters providing the estimates of the three external forces components.

4.1 NonLinear Geometric Approach

This subsection recalls the NLGA, formally developed in De Persis and Isidori [2001], on which the filters design methodology is based. For a comprehensive detailed application of the NLGA, please referee to Bonfé et al. [2011]. More precisely, the approach considers a nonlinear system model in the form:

$$\begin{cases} \dot{x} = n(x) + g(x)\,u + l(x)\,f + p(x)\,d_f \\ y = h(x) \end{cases} \tag{25}$$

in which $x \in \mathcal{X} \subset \mathcal{R}^{\ell_n}$ is the state vector, $u(t) \in \mathcal{R}^{\ell_u}$ is the control input vector, $f(t) \in \mathcal{R}$ is the external force component to be estimated, $d_f(t) \in \mathcal{R}^{\ell_d}$ the disturbance vector embedding the remaining external force components to be decoupled, $y \in \mathcal{R}^{\ell_m}$ the output vector, $n(x)$, $l(x)$, the columns of $g(x)$ and $p(x)$ are smooth vector fields, and $h(x)$ is a smooth map.

Thanks to the NLGA coordinate change the following $\bar{x}_1$–subsystem of (25) can be singled out

$$\begin{cases} \dot{\bar{x}}_1 = n_1(\bar{x}_1, \bar{y}_2) + g_1(\bar{x}_1, \bar{y}_2)\,u + \\ \qquad +l_1(\bar{x}_1, \bar{y}_2, \bar{x}_3)\,f \\ \bar{y}_1 = h(\bar{x}_1) \end{cases} \tag{26}$$

where $\bar{y}_2$ are measures of the remaining states of (25). It is worth observing that (26) is affected by the external force f and decoupled from the disturbance vector d_f. The properties of this input affine subsystem are exploited in following sub-sections, for designing of the RBF-NN adaptive filters providing external disturbance estimation.

4.2 Radial Basis Function Neural Network

Radial Basis Function Neural Network can be exploited to model and estimate generic time signals, see Buhmann [2003] and Baldi et al. [2013a]. As stated in Chen and Chen [1995] [Theorem 2], for a sufficiently large number of hidden-layers neurons, N, and if the system state $\mathbf{x} \in X \subset \mathcal{R}^{\ell_n}$, an optimal constant weight matrix W can be determined such a the continuous function, $F(t)$, can be approximated by RBFs, with a guaranteed finite model error, ε_m:

$$\left|F(x) - W^T\varphi(x)\right| = \left|F - \sum_{k=1}^{N} w_k\varphi_k(x)\right| = |e_m| < \varepsilon_m \tag{27}$$

where x is the variable on which the RBFs are defined, φ_k is k–th radial basis function and e_m is the model error between the actual function and its optimal RBF approximation. In this paper, the RBFs are assumed to be modelled as Gaussian functions as follows:

$$\varphi_k(x) = \exp(-|x - \mu_k|^2 \big/ \sigma_k^2) \tag{28}$$

where μ_k and σ_k are the center and the width of the k–th radial basis function respectively.

4.3 Design of the NLGA RBF-NN Adaptive Estimation Filters

Thanks to the NLGA procedure, three input affine $\bar{x}_1$–subsystems have been derived from the model (1) to estimate F_x, F_y and F_z .

A critical point is the estimation of generic shape external forces. To this aim the radial basis functions neural network seems to be particularly suitable, since they do not require any a priori information on the external forces internal model.

Starting from (26), an estimation filter based on RBF-NN can be modelled in the following form:

$$\begin{cases} \dot{\xi} = n_1(\bar{y}_1, \bar{y}_2) + g_1(\bar{y}_1, \bar{y}_2)\, u + \hat{F} \\ \qquad + K(\bar{y}_{1s} - \xi) \\ \varepsilon = \bar{y}_{1s} - \xi \end{cases} \tag{29}$$

where $K > 0$ represents the filter gain, which can be designed such that the residual generator (29) is asymptotically stable with a good fault sensibility vs noise attenuation ratio. Finally, the term $\hat{F}$ represents the estimation of $\ell_1(\bar{y}_1, \bar{y}_2)\, f$.

The function, $F(t)$, is estimated by the following RBF-NN:

$$\hat{F} = \hat{W}^T \varphi(\xi) \tag{30}$$

with the weight matrix $\hat{W}$ determined by the following adaptive law:

$$\dot{\hat{W}} = \eta D \varepsilon \varphi(\xi) \tag{31}$$

where $\eta > 0$ is the learning ratio and D is a proper constant matrix such that the adaptive filter (29) is asymptotically stable and the estimation $\hat{f}$ is quickly convergent to the true value.

The designed scalar NLGA RBF-NN adaptive filter providing external disturbance $\hat{F}_x$ estimate has been obtained as follows:

$$\begin{cases} \dot{\xi}_x = -\dfrac{1}{M} u_f e_1' R(q)\mathbf{e}_3 + \hat{F}_x + K_x \varepsilon_x \\ \\ \varepsilon_x = \ddot{p}_x - \xi_x \end{cases} \tag{32}$$

with the external disturbance estimation, $\hat{F}_x$, given by the relations (30), (31). The estimates of F_y and F_z can be obtained analogously.

The estimation error boundedness can be assessed by means of Lyapunov function and following the same steps made in Zhenhua et al. [2011].

5. SIMULATION RESULTS

Simulation results highlight the controller performance both with and without the exogenous disturbance estimation feedback. The simulator implements the disturbance described in Section 2.1 and an accurate wind field model. It is constituted by the following concurrent contributions: a Dryden turbulence (with zero mean), a wind shear model (to model mountain environments) and a discrete wind gust ($1 - \cos$ shape) (to take into account for asymptotically constant wind).

In the following simulation, the control objective is, starting from an erroneous initial position, a hovering at coordinates $p = [0, 0, 0]'$. During the simulated maneuver (in presence of wind) the quad–rotor is subject to external unmodeled disturbances that can affect the control accuracy both during the transient and asymptotically. Figure 1 shows the estimation filters performance in terms of both accuracy and readiness.

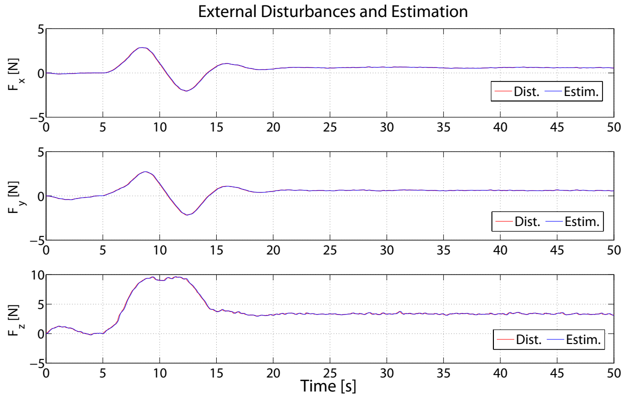

Fig. 1. Exogenous disturbance and its estimation.

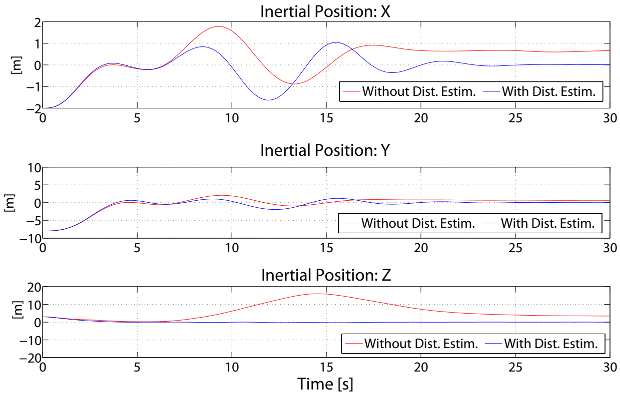

Fig. 2. Inertial position in the case of the controller with and without disturbances compensation.

The benefits arising from the feedback of the estimated exogenous disturbances are highlighted in Figures 2 and 3. During the transient flight without the estimation feedback, the z–inertial axes position time-history in Figure 2 shows an error of about 15 meters (red line) that can be reduced at about 0.50 meter (blue line). Same observations can be done by observing the figure 3.

The compensation of external disturbances can be also useful to compensate constant wind induced position error. As can be seen in Figure 2, the implemented nominal controller (without estimation feedback, red line) is not able to compensate constant external disturbances. The feedback of exogenous signal estimations allows to reach without error the target position.

6. CONCLUSION

In this paper a novel adaptive and robust controller for a quad rotor has been developed. With respect to previous contributions, such as Naldi et al. [2013] and Marconi and Naldi [2007], the position controller has been extended to take advantage from the adaptive estimation of the aerodynamic disturbances in the definition of the desired control force vector. The adaptive estimation of the exoge-

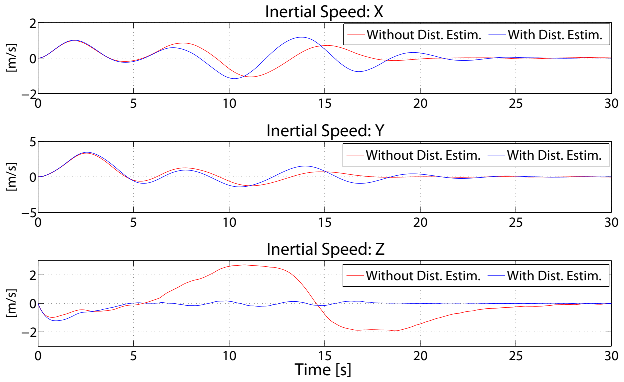

Fig. 3. Inertial speed in the case of the controller with and without disturbances compensation.

nous disturbances (aerodynamics and model mismatches) has been obtained by using the tools of the NonLinear Geometric Approach and Radial Basis Function. The robustness property of the controller guarantees the stability even in presence of estimation errors. The overall controller structure allows good tracking performances both in transient and asymptotically. The stability and the estimation performances have been showed both theoretically and in simulation.

REFERENCES

A. Abdessameud and A. Tayebi. Global trajectory tracking control of VTOL-UAVs without linear velocity measurements. *Automatica*, 46(4):1053–1059, April 2010.

P. Baldi, P. Castaldi, N. Mimmo, A. Torre, and S. Simani. A new longitudinal flight path control with adaptive wind shear estimation and compensation. *50th IEEE Conference on Decision and Control and European Control Conference*, 2011.

P. Baldi, P Castaldi, N. Mimmo, and S. Simani. Satellite attitude active FTC based on geometric approach and rbf neural network - fault tolerant control for aerospace applications. *2nd International Conference on Control and Fault-Tolerant Systems, SysTol2013*, 2013a.

P. Baldi, P. Castaldi, N. Mimmo, and S. Simani. A new aerodynamic decoupled frequential FDIR methodology for satellite actuator faults. *International Journal of Adaptive Control and Signal Processing*, DOI: 10.1002/acs.2379, 2013b.

M. Bonfé, P. Castaldi, N. Mimmo, and S. Simani. Active fault tolerant control of nonlinear systems: The cart-pole example. *International Journal of Applied Mathematics and Computer Science*, 21(3):441–445, 2011.

M. D. Buhmann. Radial basis functions: Theory and implementations. ISBN: 9780521633383, 2003.

David Cabecinhas, Rita Cunha, and Carlos Silvestre. A nonlinear quadrotor trajectory tracking controller with disturbance rejection. *Control Engineering Practice*, 26: 1–10, 2014.

P. Casau, R.G. Sanfelice, R. Cunha, D. Cabecinhas, and C. Silvestre. Global trajectory tracking for a class of underactuated vehicles. In *Proceedings of American Control Conference*, pages 419–424, Washington, US, 2013.

P. Castaldi, W. Geri, S. Simani, M. Bonfé, and M. Benini. Design of residual generators and adaptive filters for the FDI of aircraft model sensors. *Control Engineering Practice*, 18(5):449 – 459, 2010.

Tianping Chen and Hong Chen. Approximation capability to functions of several variables, nonlinear functionals, and operators by radial basis function neural networks. *IEEE Ttransactions on Neural Networks*, 6(4):904–910, 1995.

C. De Persis and A. Isidori. A geometric approach to nonlinear fault detection and isolation. *IEEE Transactions on Automatic Control*, 45(6):853–865, 2001.

E. Feron and E.N. Johnson. Aerial robotics. In B. Siciliano and O. Khatib, editors, *Springer Handbook of Robotics*, pages 1009–1027. Springer, 2008.

E. Frazzoli, M. Dahleh, and E. Feron. Trajectory tracking control design for autonomous helicopters using a backstepping algorithm. *Proceedings of the American Control Conference*, pages 4102–4107, 2000.

J. Hauser, S. Sastry, and G. Meyer. Nonlinear control design for slightly non-minimum phase systems: application to V/STOL aircraft. *Automatica*, 28(4):665–679, 1992.

M. Hua, T. Hamel, P. Morin, and C. Samson. Introduction to feedback control of underactuated VTOL vehicles. *IEEE Control Systems Magazine*, 33(2):61–75, February 2013.

M.D. Hua, T. Hamel, P. Morin, and C. Samson. A control approach for thrust-propelled underactuated vehicles and its applications to VTOL drones. *IEEE Transsactions on Automatic Control*, 54(8):1837–1853, 2009.

A. Isidori, L. Marconi, and A. Serrani. *Robust Autonomous Guidance: An Internal Model Approach.* Advances in Industrial Control. Springer-Verlag London, 2003.

R.E. Mahony, V. Kumar, and P. Corke. Multirotor aerial vehicles: Modeling, estimation, and control of quadrotor. *IEEE Robot. Automat. Mag.*, 19(3):20–32, 2012.

L. Marconi and R. Naldi. Robust nonlinear full degree of fredom control of an helicopter. *Automatica*, 42:1584–1596, 2007.

L. Marconi and R. Naldi. Control of aerial robots. hybrid force/position feedback for a ducted-fan. *IEEE Control System Magazine*, 32(4):43–65, 2012.

L. Marconi, R. Naldi, and A. Isidori. High-gain output feedback for a miniature UAV. *International Journal of Robust and Nonlinear Control*, 2013. doi: doi:10.1002/rnc.2959.

P. Martin, S. Devasia, and B. Paden. A different look at output tracking: control of a VTOL aircraft. *Automatica*, 32(1):101–107, 1996.

C. Mayhew, R. Sanfelice, and A. Teel. On path-lifting mechanisms and unwinding in quaternion-based attitude control. *IEEE Transactions on Automatic Control*, 58(5):1179–1191, 2012.

R. Naldi, M. Furci, R.G. Sanfelice, and L. Marconi. Global trajectory tracking for underactuated VTOL aerial vehicles using a cascade control paradigm. In *Proc. of IEEE Conference on Decision and Control*, Florence, IT, 2013.

M.D. Shuster. A survey of attitude representation. *The Journal of the Astronautical Sciences*, 41(4):439–517, December 1993.

Wang Zhenhua, Shen Yi, and Zhang Xiaolei. Actuator fault detection and estimation for a class of nonlinear systems. In *Seventh International Conference on Natural Computation*, 2011.